NATIONAL AERONAUTICS AND SPACE ADMINISTRATION

Technical Report 32-1297

Performance of a Breadboard Electronics System Developed for a Lunar Orbiter Gamma Ray Spectrometer

Albert E. Metzger

JET PROPULSION LABORATORY
CALIFORNIA INSTITUTE OF TECHNOLOGY
PASADENA, CALIFORNIA

October 1, 1968

NATIONAL AERONAUTICS AND SPACE ADMINISTRATION

Technical Report 32-1297

Performance of a Breadboard Electronics System Developed for a Lunar Orbiter Gamma Ray Spectrometer

Albert E. Metzger

Approved by:

Robert J. Mackin, Jr., *Manager*
Lunar and Planetary Sciences Section

JET PROPULSION LABORATORY
CALIFORNIA INSTITUTE OF TECHNOLOGY
PASADENA, CALIFORNIA

October 1, 1968

TECHNICAL REPORT 32-1297

Prepared Under Contract No. NAS 7-100
National Aeronautics & Space Administration

Acknowledgments

Tim Harrington, James Ferris, Rex Shields, and Lanny Lewyn participated in the testing. Louis Huszar wrote the computer program for the reduction of the digital output data. Richard Parker and Sally Rubsamen assisted in data reduction. James Arnold, Robert Hollman, and Ernest Franzgrote kindly contributed the use of their respective Nuclear Data 130 pulse-height analyzers during periods of need. The data translator and tape deck were loaned by Laurence Peterson; Paul Brissenden assisted in preparing them for use.

Contents

I. Introduction 1

II. Description 2

III. Test Results 4

A. Integral Nonlinearity 4

B. Differential Nonlinearity 6

C. Channel Resolution 6

D. Zero Offset 8

E. Gain Stability 8

F. High-Voltage Stability 8

G. Thermal Test 9

H. Resolution 9

I. Peak Position Linearity 9

J. Count Rate Stability 10

K. Overload Recovery and Shield Test 10

L. Pulse Pair Resolution 12

M. Digital Readout Logic and Scaler Functions 12

N. Miscellaneous 14

IV. Summary 14

Appendix Tests at the Oak Ridge National Laboratory 15

Tables

1. Channel resolution 7

2. Zero offset stability 8

3. Gain stability 9

4. High-voltage regulation 9

5. Thermal stability 11

6. Characteristic energies of measured spectra 11

7. Count rate stability (I) 11

8. Effect of veto action on spectral distribution 12

Contents (contd)

Tables (contd)

A-1. Overload recovery 17
A-2. Count rate stability (II) 17

Figures

1. Block diagram of gamma ray spectrometer breadboard 3
2. Photograph of breadboard unit 4
3. Plot of incremental inputs 5
4. Integral linearity 5
5. Differential linearity (I) 6
6. Channel profile 7
7. Variation with time 8
8. Spectrum of Cs-137 10
9. Plot of photopeak energies vs channel number 11
10. Digital output format 13
A-1. Differential linearity (II) 15
A-2. Veto action 16

Abstract

An electronics system intended to be part of a remote-sensing gamma ray spectrometer has been designed and constructed. This report describes the system and a series of evaluation tests performed on the breadboard model. Results of the test program have been satisfactory, leading to the construction of a space-hardened prototype.

Performance of a Breadboard Electronics System Developed for a *Lunar Orbiter* Gamma Ray Spectrometer

I. Introduction

Experiments designed to measure the gamma ray flux emitted from the surface of the moon have been recognized for a number of years as a potentially valuable indicator of the moon's thermal history. In April 1966, the feasibility of the technique was confirmed in practice by a gamma ray spectrometer which made successful observations from the *Luna 10* orbiting spacecraft. Following the second successful flight of the Langley–Boeing *Lunar Orbiter* in the fall of 1966, the Office of Space Science and Applications at NASA expressed interest in the possibility of placing a gamma ray spectrometer on the fifth and last flight of this series of missions.

After the initial meeting with project representatives at the Langley Research Center and an assessment of the *Orbiter's* capabilities, the potential experimenters (J. R. Arnold and L. E. Peterson of the University of California–San Diego, J. I. Trombka of the Goddard Space Flight Center, and A. E. Metzger of the Jet Propulsion Laboratory) made the following decisions: (1) that the flight equipment remaining from the *Ranger* Project, which had carried a gamma ray spectrometer on three missions in 1961–1962, was too outdated to provide a state-of-the-art experiment; and therefore (2) that electronics breadboards would be designed and fabricated by two experienced contractors while the Boeing Corp., as prime contractor for the *Lunar Orbiter* program, was evaluating the interfaces between the instrument and the spacecraft; and (3) that the bandwidth available for photographic transmission made it possible to transmit the gamma ray data essentially in real-time. Eliminating the need for spacecraft data compression permitted a substantial simplification of the instrument with a shortened developmental schedule. On the other hand, it precluded obtaining any data from portions of the lunar surface viewed when the spacecraft was not in line of sight of the earth.

The electronics breadboards were designed and constructed by the Analog Technology Corp. (ATC), Pasadena, California, and Space and Tactical Systems, Inc., Nashua, New Hampshire, under contract to the University of California–San Diego (UCSD) and the Goddard Space Flight Center (GSFC), respectively. The ATC system was delivered to the Jet Propulsion Laboratory (JPL) for testing on January 24, 1967. The following sections present a brief description of the functions of this breadboard and the results of tests subsequently performed at JPL. The ATC instrument was also one of three pulse-height analysis systems designed for use in space

which was subject to a series of comparative tests at the Oak Ridge National Laboratory (ORNL) from July 20–27, 1967. By this time it had been decided that the development and integration of a gamma ray spectrometer for the last *Lunar Orbiter* mission would impose too great a delay on the launch of that vehicle. The tests at ORNL reflected a general recognition by NASA and interested scientists that this type of instrumentation will be needed in the future for a variety of experiments utilizing such techniques as neutron analysis, alpha scattering, nondispersive X-ray spectroscopy, particle spectroscopy, etc., in the fields of astrophysics and planetology. The results of the ORNL tests on the ATC breadboard are presented in an appendix.

II. Description

A gamma ray spectrometer consists of a detector, high-voltage supply, amplifiers, coincidence gate, analog-to-digital converter, shift register, magnetic core memory or tape storage if data compression is required, and telemetry encoding logic. The most suitable detector for use at this time consists of a large crystal of thallium-activated sodium iodide [NaI (Tl)] which is optically coupled to a photomultiplier tube. Gamma rays are stopped in the NaI (Tl) crystal, and the resulting light output of the scintillation crystal is sensed by the photocathode of the associated photomultiplier tube. The scintillating plastic which surrounds the NaI (Tl) crystal and is viewed by a second photomultiplier tube serves as an anticoincidence shield for the rejection of charged particles.

The block diagram of the ATC pulse height analyzer (PHA) is shown in Fig. 1. A charge-sensitive preamplifier receives current pulses from the anode of the photomultiplier which is coupled to the NaI (Tl) crystal. These pulses are amplified and shaped before being digitized by the analog-to-digital converter (ADC), which includes a linear gate and offset circuit, a height-to-time converter (HTC), a 1-MHz crystal clock oscillator, and clock gating circuits. The input pulse charges a capacitor in the HTC, the discharge of which produces a pulse proportional to the input pulse amplitude. During the discharge, the number of pulses from the crystal clock oscillator is gated into an 8 bit address scaler permitting 255 channels of analysis. An analysis does not take place if a pulse from the shield scintillator exceeds the threshold of the shield discriminator or if the HTC is still processing a previous event.

Three scalers are included in the breadboard. These supply additional data for the experiment and provide checks on the proper operation of the instrument. The veto events scaler counts events which produce coincidence pulses in the shield scintillator and the NaI crystal. These are not analyzed. The busy events scaler counts pulses from the NaI crystal which are not analyzed because the ADC or the telemetry system is occupied with a previous event. Although the busy scaler does not count all events during the time the linear gate of the ADC is closed, a dead time correction can be made from the spectral distribution and the busy scaler rate. The shield scaler registers all pulses from the shield scintillator which exceed the discriminator level. The shield scaler gives the value of the charged particle flux. All three scalers switch from a count to a time-to-overflow mode when the contents of the scaler exceed 216 counts. This switching expands the dynamic range of the scalers. In the time-to-overflow mode, the time which has been required to accumulate 216 counts is measured by counting at a 660-Hz clock rate.

After a digital event is counted in the address scaler it is transferred to a buffer register for readout. The digital readout system was designed to take advantage of the wideband telemetry channel used for transmitting photographic data on the *Lunar Orbiter*. The format consists of 128 9 bit words which comprise a frame. The first five words are devoted to a 43 bit Legendre code for synchronization. The next four words contain the contents of the three scalers. Each of the scaler functions is assigned one word. The fourth word is encoded so as to show whether any of the scalers are counting in the time-to-overflow mode. The remaining words, from 10 through 128, are available for pulse-height data. Each scaler and pulse-height analysis word contains 8 data bits and 1 parity bit. The transmission rate of 3906 bits/sec is derived by scaling down the 1-MHz crystal clock oscillator by a factor of 256. This fixes the readout periods of 0.256 millisec/bit, 2.30 millisec/word, and 292 millisec/frame. The average maximum rate for spectral analysis is, therefore, $(118/128)\ (1/2.30 \times 10^{-3}) = 402$ counts/sec. This is adequate for nominal lunar and cislunar conditions with a $2\frac{3}{4} \times 2\frac{3}{4}$-in. scintillation crystal in the detector. Higher count rates would result in a partial loss of data, but a dead-time correction can be made.

The command capability of the breadboard includes power on/off, shield veto disable, and a 3 bit (8 position) high-voltage step command which permits the programming of seven levels of voltage plus a zero position. The

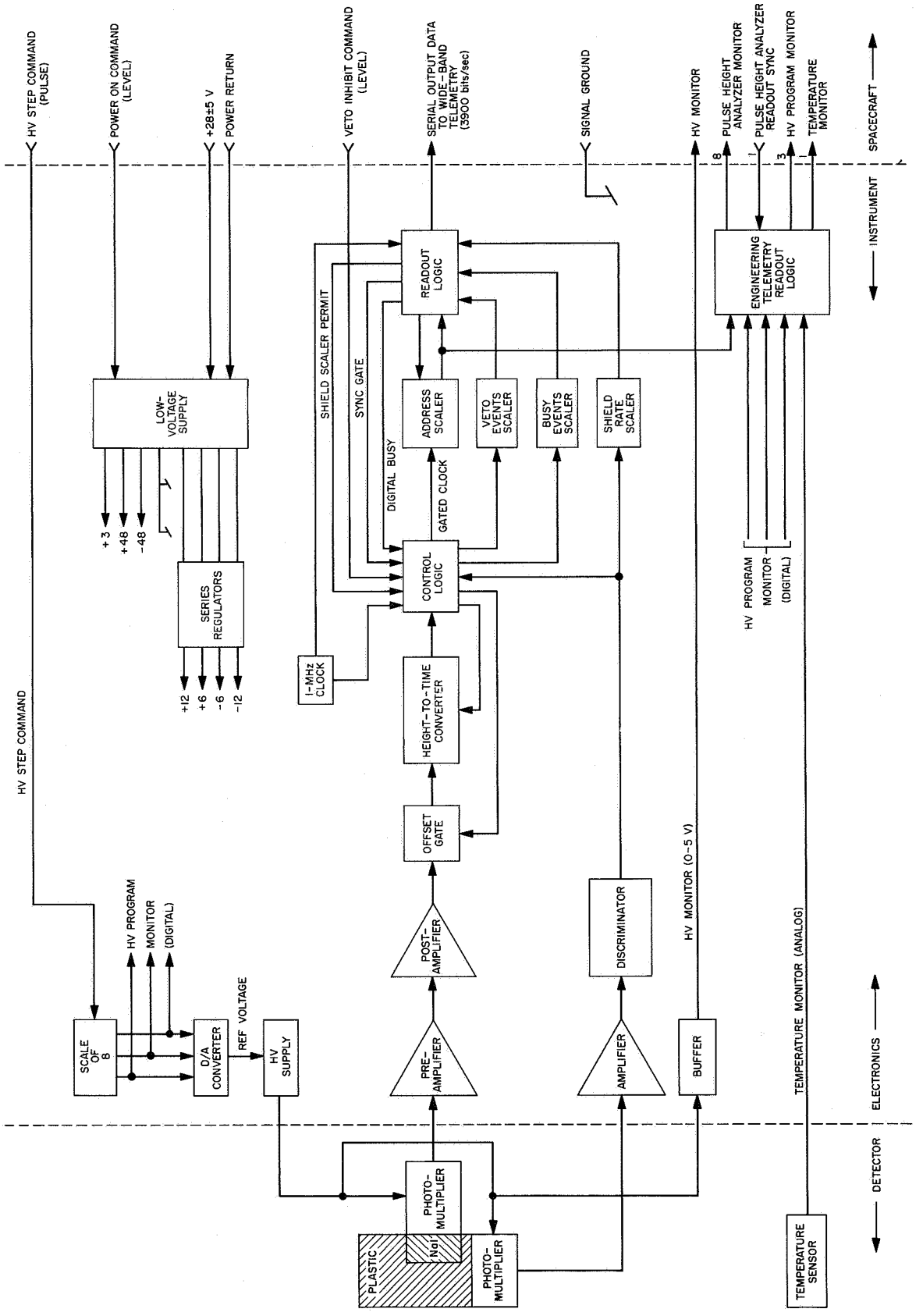

Fig. 1. Block diagram of gamma ray spectrometer breadboard

high-voltage step command is intended to make adjustments in gain as necessary during the flight. It functions through a digital-to-analog converter which produces the reference voltage for the supply. One high-voltage supply is used for both detector photomultiplier tubes, although the tubes will probably not operate at the same voltage.

Besides the main data readout system just described, the breadboard makes provision for the readout of certain engineering data. These data are shown in Fig. 1, and include the high-voltage output, the state of the high-voltage step command, and a thermistor. There is also an 8 bit PHA monitor which allows the receipt of a limited amount of spectral data or serves as a functional check during periods when the main data channel is not available to the experiment.

A photograph of the breadboard unit is shown in Fig. 2.

III. Test Results

No specific bench check or ground support equipment was constructed with which to decode and present data formated in the digital readout electronics. It was necessary to frame-sync the digital output in a buffer decoder, from which it was transmitted to a tape recorder. The tape was translated and reduced in an IBM 7090 computer, using a program written for this purpose. Because of the delays involved and the limited availability of a tape deck and translator, most of the tests were performed by simply accumulating the output of the address scaler in the memory of a Nuclear Data Corp. model 130 pulse-height analyzer. Except for the tests of the digital readout logic, all the results presented below were obtained in this manner.

A. Integral Nonlinearity

Integral nonlinearity was measured with a digital-to-analog converter (DAC) test system which employs a stable voltage source, precision digital-to-analog voltage divider to present signals of accurately known amplitude to the breadboard input. The voltage level is controlled by means of a binary counter. The number of steps and the stepping rate are chosen by selecting the desired binary switches and the instrument sequences repetitively. In this test, 64 steps were used at a stepping rate of approximately 1 per sec. An Ortec model 204 pulse generator provided the output pulses. A sine-wave generator with a 50-ohm resistor placed from signal to ground was used at the DAC output to produce enough peak broadening in the input signal to smear each point across two channels of digital address. This permitted a more accurate determination of peak position. Figure 3 shows the measured channel number as a function of the input pulse increment. Figure 4 shows the deviation in channels from a straight line for each point measured.

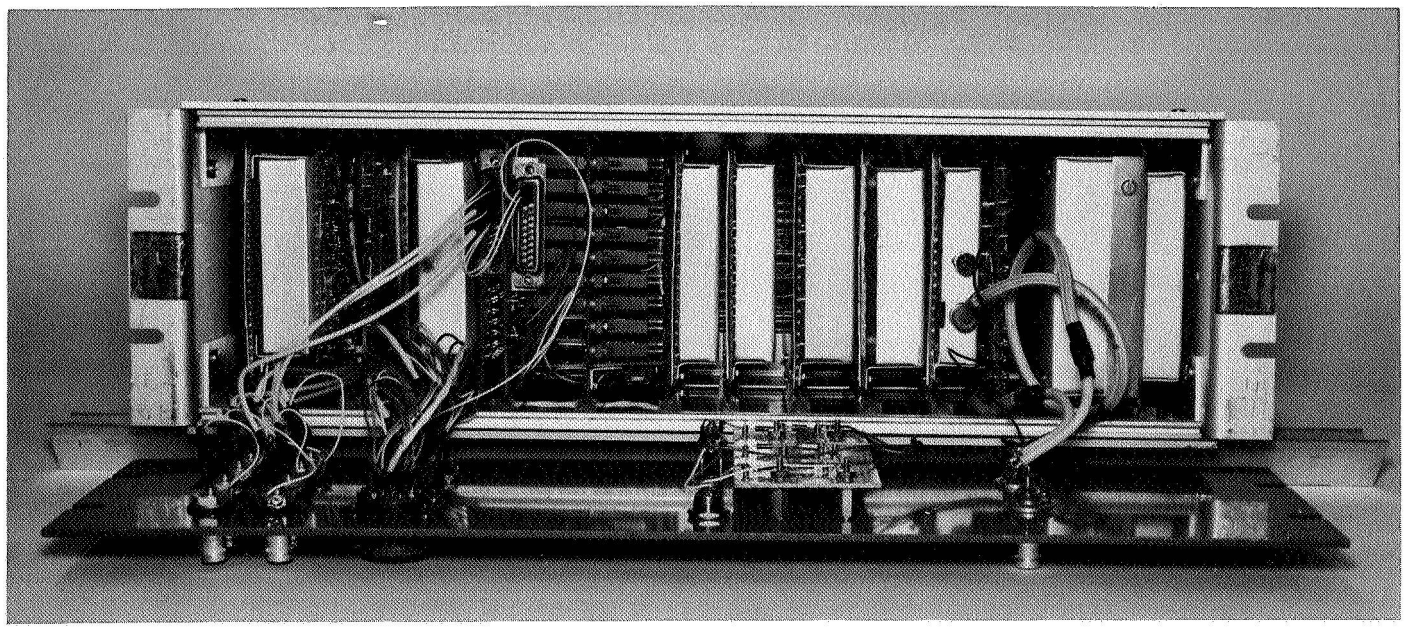

Fig. 2. Photograph of breadboard unit

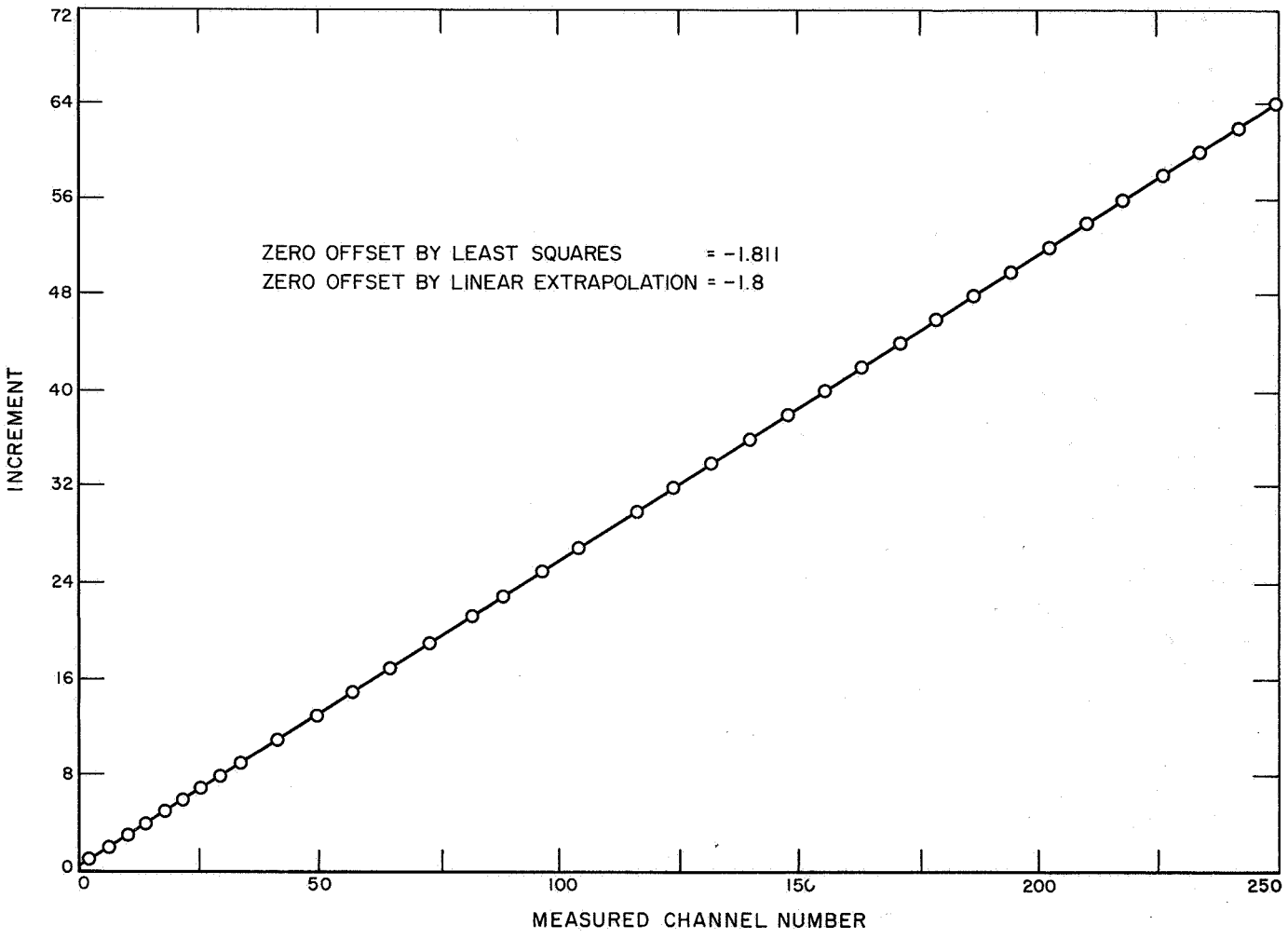

Fig. 3. Plot of incremental inputs

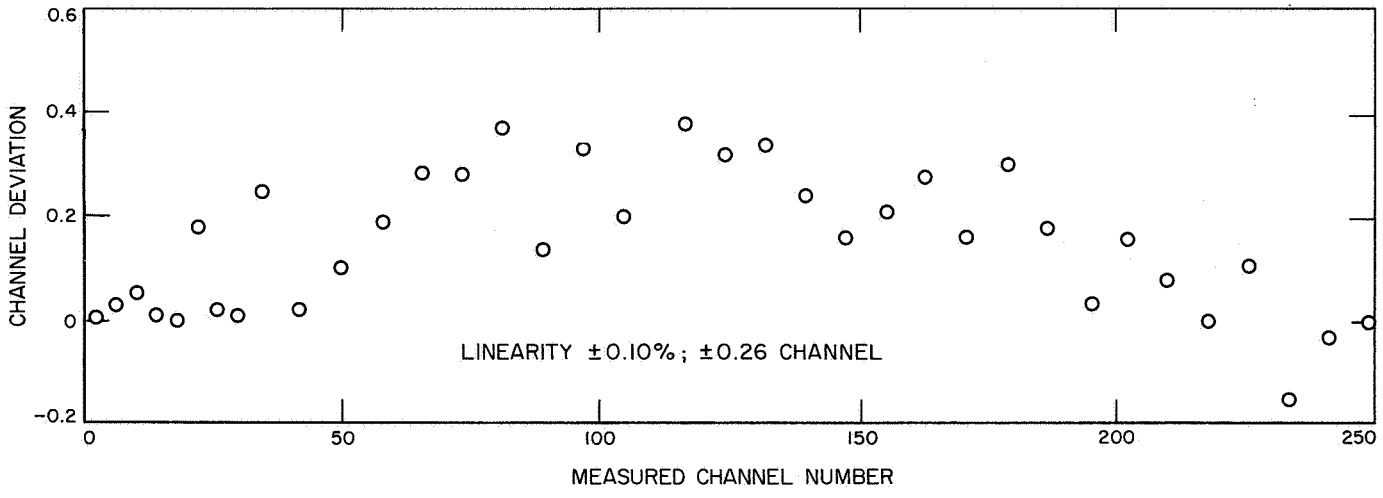

Fig. 4. Integral linearity

The maximum deviation from linearity is ± 0.26 channels. Using the customary convention, i.e., the percent deviation in channels from a straight line divided by the maximum number of channels, this corresponds to an integral nonlinearity of 0.52/255 = 0.20% or ± 0.10%. The maximum deviation at any particular channel was 0.38/116 = 0.44%. Measurements of integral nonlinearity before and after thermal testing were in good agreement.

B. Differential Nonlinearity

Differential nonlinearity defines the uniformity of channel width across the conversion range of a pulse-height analyzer. It was measured by using all 4096 precision levels of the DAC test system across the 255 channels of analysis in the breadboard. The variation of individual channel widths is reflected in the number of counts deposited in each channel. The data are shown in Fig. 5. Channels 130 and 196 have high values which must be due to a spurious effect, possibly line transients. They have been disregarded. The maximum deviation from the average number of counts in each channel for the remaining channels is +2.66% and −1.17%. The much higher deviation in the positive direction suggests that spurious counts have been added to channels other than the two already discounted. A close examination of the data also indicates the existence of an alternating channel count effect due to the narrow width of pulses out of the DAC test system and the sharp channel boundaries of the breadboard. Differential nonlinearity was also measured with a Berkeley Nuclear Corp. (BNC) PB-2 pulse generator and a Tectronics Inc. model 535 oscilloscope. This combination generates a continuously varying ramp of pulses. A problem in the test equipment led to unsatisfactory results. A good measurement of differential nonlinearity was obtained during the tests at ORNL with a BNC-GL-3 ramp pulse generator. The differential nonlinearity measured at ORNL was ± 0.66% (see Appendix and Fig. A-1).

C. Channel Resolution

The ability of the breadboard PHA to resolve signals between adjacent channels was determined by measuring the channel address as a function of input pulse amplitude. The input pulses were generated using the precision voltage divider of the DAC test system and the Ortec pulser. The input voltages were carefully read on a Dymec[1] model DY-2401B integrating digital voltmeter. Each run was for 1 min, providing 60 pulses/sec × 60 sec × 119/128 = 3350 counts for analysis. A plot of the results for the pair of boundaries separating channels 128–129 and 129–130 is shown in Fig. 6.

A total of eight such pairs were mapped across the 255 channels of pulse-height analysis to determine channel resolution. Channel resolution is defined here as the ratio of the channel width within which a given fraction of counts is found, divided by the full width of the

[1]Division of Hewlett-Packard Co.

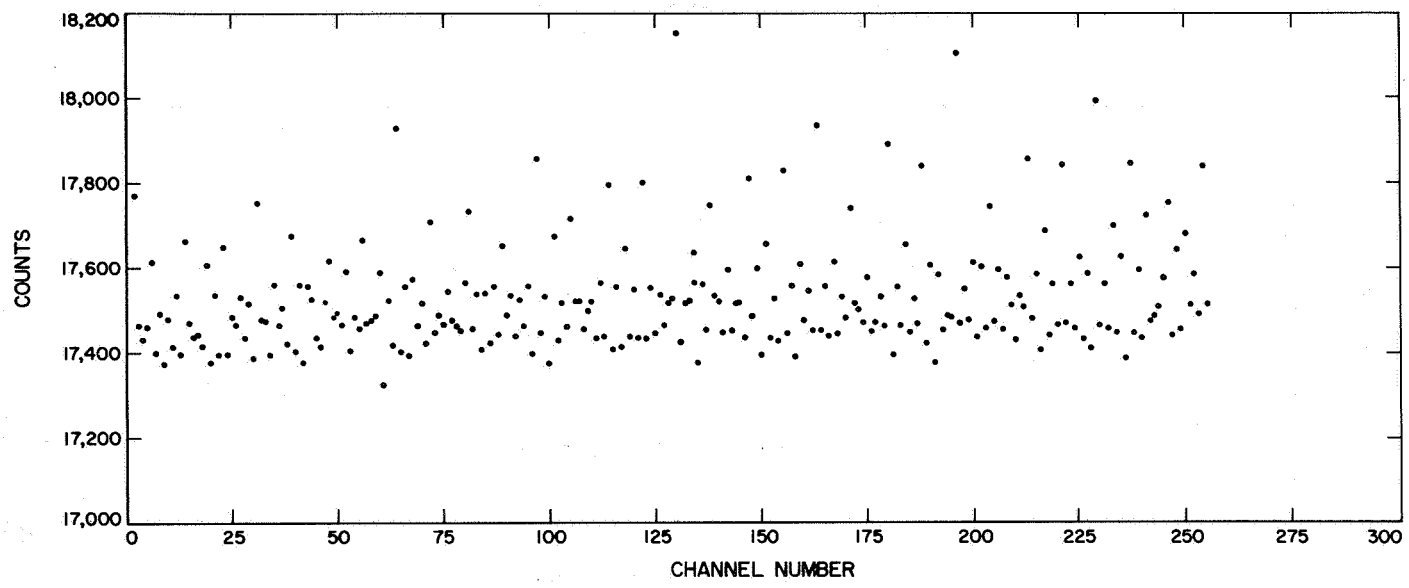

Fig. 5. Differential linearity (I)

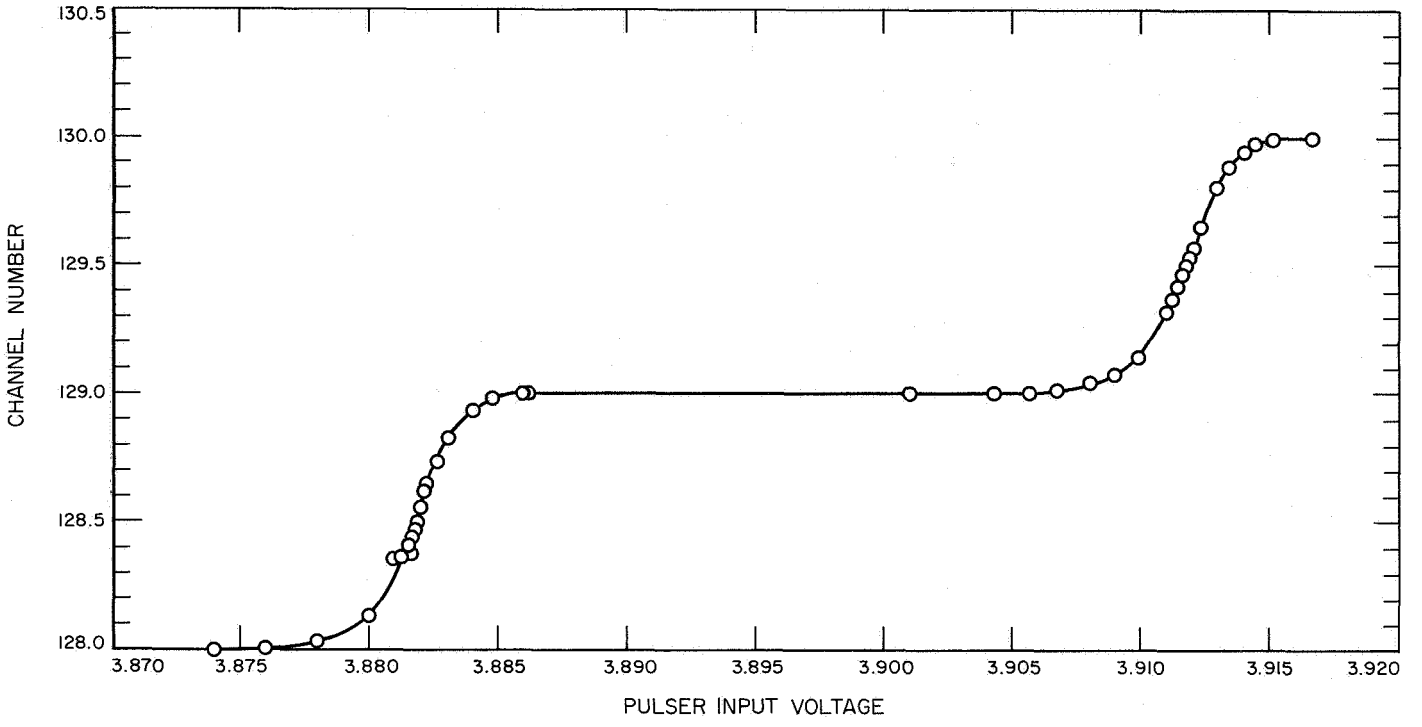

Fig. 6. Channel profile

channel as measured between the midway points of a pair of channel boundaries. Thus in Fig. 6 the 90% resolution of channel 129 is the input voltage differential between channel 128.95 and channel 129.05 divided by the input voltage differential for the full channel width, i.e., from channel 128.50 to channel 129.50. The measured values for channel resolutions of 90% and 98% are given in Table 1. The channel boundaries are sharp. There is a small decrease in resolution with increasing channel number, amounting to about 7% over the conversion range. Note that the HTC can count to approximately channel 275, although 255 is the limiting number of channels which the address scaler can transmit to the digital electronics.

Table 1. Channel resolution

Upper boundary		Lower boundary		Full channel width ($V_u - V_l$), V	90% channel resolution (R_{90})[a]	98% channel resolution (R_{98})[b]
Channel	Pulser voltage V_u, V	Channel	Pulser voltage V_l, V			
6.50	0.2547	5.50	0.2249	0.0298	0.839	0.735
28.50	0.8715	27.50	0.8429	0.0286	–	–
64.50	2.0084	63.50	1.9783	0.0301	0.814	0.724
129.50	3.9118	128.50	3.8818	0.0300	0.807	0.723
160.50	4.8452	159.50	4.8149	0.0303	0.789	0.700
192.50	5.8044	191.50	5.7745	0.0299	0.789	0.736
226.50	6.8480	225.50	6.8178	0.0302	0.778	0.692
257.50	7.8069	256.50	7.7766	0.0303	0.805	0.683

[a] $R_{90} = \frac{\text{width from channel } (x - 0.05) \text{ to channel } (x + 0.05)}{\text{full channel width}}$

[b] $R_{98} = \frac{\text{width from channel } (x - 0.01) \text{ to channel } (x + 0.01)}{\text{full channel width}}$

In Table 1, $V_u - V_l$ is also a measure of differential nonlinearity. Ignoring the data for channels 27–29, which is sketchy, the channel width values are uniform across the full range. The variation of ±1–2% is in general agreement with the differential nonlinearity measurement discussed previously.

D. Zero Offset

Zero offset is the intercept on the ordinate of the best linear fit between energy and channel number. In order to accurately assign the characteristic energy to a given peak position, the value of zero offset must be known. Drifts in zero offset are therefore undesirable. The zero offset was determined with the DAC test unit by measuring the channel values of a set of known input amplitudes, making a least squares linear fit, and extrapolating to zero pulse amplitude as shown in Fig. 2. Table 2 lists all measurements of zero offset made at room temperature. Variations in zero offset are referenced to the value obtained on 2/28/67 at 1100 hours. The change in zero offset between 2/28/67 and 3/13/67 is plotted in Fig. 7a. The relatively large excursion on 3/1/67 is considered real. From Table 2 it is seen that the shift in zero offset did not exceed 0.4 channels over a period of 4½ months. No internal adjustments affecting zero offset were made to the breadboard during this period.

Table 2. Zero offset stability

Date, 1967	Time	Zero offset, channel	Zero offset drift, channel
2/28	1100	−2.0079	0
	1230	−2.0100	−0.0021
	1300	−2.0040	0.0039
	1330	−2.0067	0.0012
3/1	0945	−1.9905	0.0174
	1110	−1.6585	0.3494
	1735	−1.9864	0.0125
3/2	0900	−2.0213	−0.0134
	1530	−1.9932	0.0147
3/3	0900	−2.0160	−0.0081
3/8	1600	−2.0040	0.0039
3/9	1400	−2.0093	−0.0014
3/13	1300	−1.9863	0.0216
3/15	1100	−1.8112	0.1967
4/29	1600	−1.9019	0.1060
6/27	—	−1.9690	0.0389

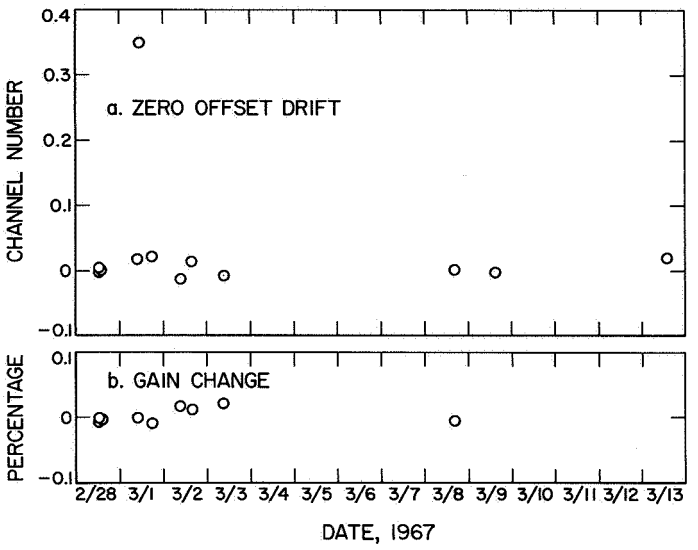

Fig. 7. Variation with time

E. Gain Stability

A constant gain over a period of time corresponding to statistically significant counting intervals is necessary to avoid degrading the energy resolution of the detector. It is also desirable over longer periods to minimize the need for commanded gain shift adjustments. The variation in gain was monitored from 2/28/67 to 3/8/67. The data are presented in Table 3 and plotted in Fig. 7b. The pulser was set initially to address at the boundary between channels 129 and 130 in order to maximize the sensitivity of this test. This reference amplitude was 3.97262 V, and each subsequent peak position measurement listed in the "channel" column was obtained at this setting. The measured peak position is corrected for changes in zero offset in the next column. The column headed "gain" gives the normalized amplitude derived from the corrected channel number and the channel profile of Fig. 6, which takes into account the nonlinearity of input amplitude with channel number. The maximum variation in gain amounted to 0.024%.

F. High-Voltage Stability

The stability of the high-voltage supply was measured by monitoring the analog output of the high-voltage monitor with a Hewlett-Packard model 405 digital voltmeter. The high-voltage monitor was sampled 7 times per min. The high voltage is related to the analog output by:

$$HV = \frac{200\beta}{1.03} + 750$$

Table 3. Gain stability

Date, 1967	Time	Zero offset, channel	Channel	Corrected channel	Gain, V	Gain change, V	Gain change, %
2/28	1230	−2.0100	129.5399	131.5499	3.97262	0	0
	1300	−2.0040	129.5125	131.5165	3.97241	−0.00021	−0.0053
	1330	−2.0067	129.5322	131.5389	3.97253	−0.00009	−0.0023
3/1	0945	−1.9905	129.5729	131.5634	3.97267	0.00005	0.0013
	1733	−1.9864	129.4978	131.4842	3.97237	−0.00025	−0.0063
3/2	0900	−2.0213	129.7551	131.7764	3.97343	0.00081	0.020
	1530	−1.9932	129.7263	131.7195	3.97323	0.00061	0.015
3/3	0900	−2.0160	129.7917	131.8077	3.97358	0.00096	0.024
3/8	1600	−2.0040	129.5201	131.5241	3.97248	−0.00014	−0.0035

Table 4. High-voltage regulation

Run	Duration, hr, min	Analog monitor, V		High voltage, V		High voltage change, V	Regulation, %
		High	Low	High	Low		
1	14:34	2.73060	2.72981	1280.21	1280.01	0.20	0.0156
2	13:55	2.73046	2.72915	1280.19	1279.93	0.26	0.0203
Combined	28:29	2.73060	2.72915	1280.21	1279.93	0.28	0.0219

where $\beta \equiv$ analog output level. The results of 28 hr of measurement at 30°C are given in Table 4. During this period the voltage regulation was better than 0.022%.

G. Thermal Test

The breadboard was placed in an oven and cycled through the following sequence: 20° to 70° to −30° to 20°C. The first time the test was attempted, the voltage regulation circuit failed at the high temperature end because insufficient allowance had been made for an increase in leakage current. This problem was corrected at ATC; the unit was returned to JPL and the test repeated. The data points were obtained in the order listed in Table 5, with a minimum of 3 hr allowed for thermal equilibration. The parameters monitored were zero offset, gain, and high voltage. Over the test range of 100°C, the maximum variation in zero offset was 0.202 channels; the maximum variation in gain was 0.19%, and the maximum variation in high voltage was 7.61 V or 0.69%. Most of the change in high voltage occurred between 30° and 8°C, indicating an irreversible shift in some component of the high-voltage regulator.

H. Resolution

A 10-microcurie (μc) source of cesium-137 was placed 24 cm from a scintillation detector. The 3-in. sodium iodide (Tl) crystal of this detector was mounted on an RCA type C31009 ceramic photomultiplier tube. The breadboard high-voltage supply was set at 1490 V. The counting times of source and background were 10 min each. Figure 8 shows the net background subtracted spectrum of Cs-137. The resolution of the peak is 8.7%, and the peak/valley ratio is 40.9. This detector system with the same source-detector geometry coupled to a laboratory amplifier high-voltage supply and pulse-height analyzer had a resolution of 8.6% and a peak/valley ratio of 24.9. The well-formed cesium K_α X-ray peak at 31.0 keV which appears in channel 5 and 6 of Fig. 8 demonstrates that the noise level in the breadboard is low. The peak in channel 14 and 15 is 75.0 keV PbK_α radiation. It is due to secondary fluorescence generated by the Cs-137 gamma ray flux incident upon lead shielding surrounding the detector.

I. Peak Position-Linearity

With the gain of the breadboard system set to span an energy range of 0–8.5 MeV, spectra were obtained from sources of cesium-137, yttrium-88, and a sample of monzonite, a mineral rich in thorium. The energies, peak positions, and rates in counts/sec of the more prominent peaks are given in Table 6, and the peak positions are

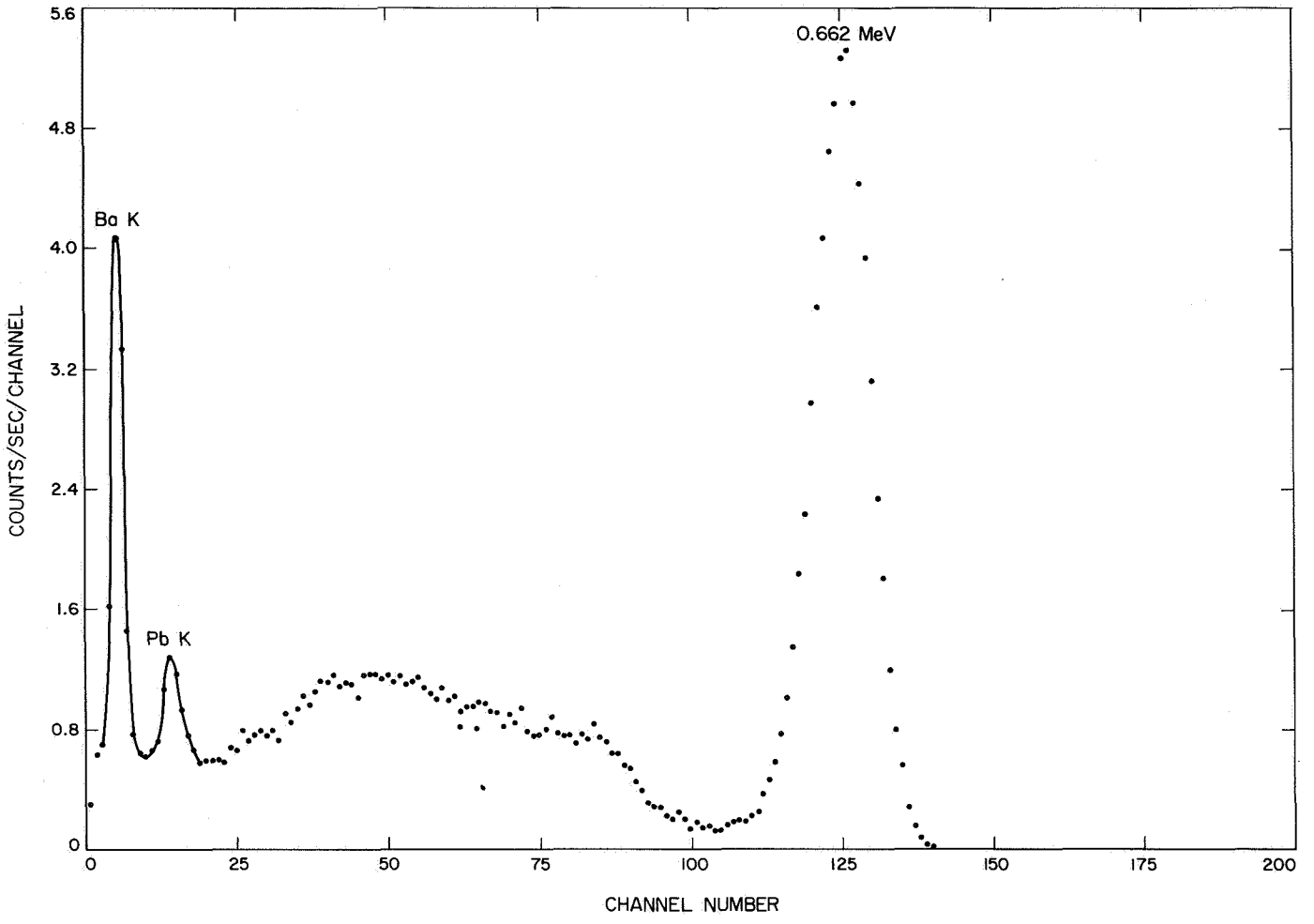

Fig. 8. Spectrum of Cs-137

plotted against energy in Fig. 9. The points define a linear relationship between incident gamma ray energy and peak position. The sodium iodide crystal used in these tests contained a small quantity of americium-241, whose alpha decay peak provides a calibration point for the spectrum. The gamma ray energy equivalent of this line had been determined as 3.06 MeV with a laboratory amplifier and PHA. The measurement with the breadboard suggests that a better value of this energy is 3.01 MeV.

J. Count Rate Stability

A measurement was made of the effect of counting rate on peak position. A Cs-137 source was positioned and counted at varying distances from the crystal. The data of Table 7 show that the peak position is unaffected by a change in counting rate from 0.1–2.6 kHz. For reasons of geometry the resolution is best at 18 cm. At greater distances the background becomes more dominant, and at closer distances scattering in the detector increases. The peak/valley ratios vary widely because of limited statistics. Note the approach of the PHA counting rate to the limiting value of 403 counts/sec.

K. Overload Recovery and Shield Test

The average cosmic ray proton of minimum ionizing energy passing through a 3 × 3-in. sodium iodide crystal will deposit on the order of 100 MeV in the crystal. Heavier particles will lose still more energy, the amount varying as the square of the charge of the cosmic ray primary. These large pulses will produce overload effects which may distort subsequent gamma ray pulses owing to a baseline shift. The overload recovery characteristics of the amplifier and ADC were first observed on a scope using pulses from a Lavoie generator. Input signal amplitudes of 25, 50, and 100 V were used; a 100 V signal

Table 5. Thermal stability

Temperature, °C	Zero offset, channel	Zero offset drift, channel	Input pulser amplitude, V	Normalized to channel 128.50 and corrected for zero offset drift, V	Gain change, %	High voltage, V	High-voltage change, %
20	−1.8677	0	3.9045	3.9065	—	1095.23	—
39	−1.9131	−0.0454	3.9042	3.9614	0.02	1096.34	0.10
60	−1.9738	−0.1061	3.9059	3.9650	0.11	1096.61	0.13
69	−2.0088	−0.1411	3.9077	3.9678	0.18	1097.04	0.17
49	−1.9313	−0.0636	3.9037	3.9614	0.02	1096.20	0.09
30	−1.9019	−0.0342	3.9033	3.9603	−0.01	1095.46	0.02
8	−1.8629	0.0048	3.9049	3.9608	0.01	1090.27	−0.45
−10	−1.8617	0.0060	3.9097	3.9656	0.13	1089.47	−0.53
−30	−1.8065	0.0612	3.9102	3.9644	0.10	1091.42	−0.35
−19	−1.9115	−0.0438	3.9087	3.9660	0.14	1090.91	−0.39
0	−1.8995	−0.0318	3.9079	3.9649	0.11	1091.08	−0.38
20	−1.9055	−0.0378	3.9057	3.9627	0.06	1089.43	−0.53

Table 6. Characteristic energies of measured spectra

Source	Energy, MeV	Peak position, channel	Peak, counts/sec
Tl-208	0.58	18.1	22.8
Cs-137	0.66	20.9	65.8
Y-88	0.91	28.2	74.5
Bi-214	1.61	50.9	4.2
Y-88	1.84	58.0	35.8
Tl-208	2.62	83.1	4.2

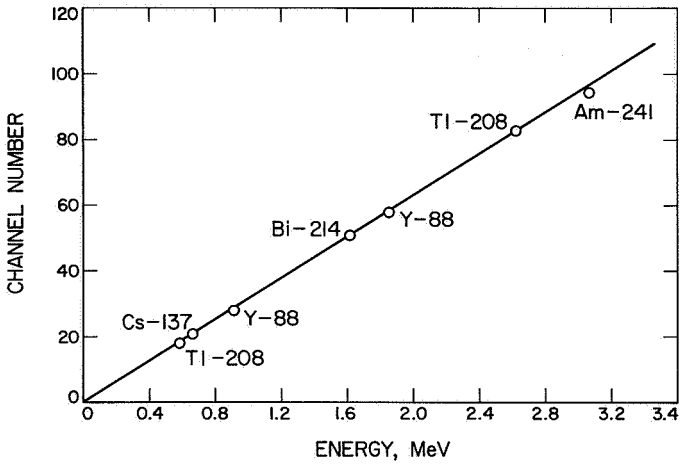

Fig. 9. Plot of photopeak energies vs channel number

Table 7. Count rate stability (I) (Cs-137 source)

Source-detector distance, cm	Incident flux, counts/sec	Peak position, channel	Resolution, %	Peak/valley	Measured flux, counts/sec
48	134	124.5	9.09	46.0	99
24	252	124.0	8.24	32.4	186
18	363	124.4	8.31	41.8	236
12	660	124.3	8.46	56.5	307
6	—	123.6	8.70	43.3	378
3	2600	124.4	8.60	51.6	394

is roughly 10 times the amplifier saturation value and in this case corresponded to the deposition of about 110 MeV of energy in the crystal. In all cases, the amplifier was observed to recover to within 5 mV, approximately 1/6th of a channel, of the baseline in 250 μsec, and the linear gate was observed to remain closed for longer than this period so that no pulse analysis could be offset by more than this amount.

In order to get higher overload factors and make a more sensitive determination of baseline shift, the pulses out of the Lavoie generator were amplified by means of a circuit designed by L. Lewyn. The Lavoie generator with overload pulse amplifier was set to supply 100 times saturation signals to the breadboard preamplifier at a

rate of 300 pulses/sec. Simultaneously, a 2-in. Harshaw integral line assembly transmitted spectral data to the overload pulse amplifier in parallel with the Lavoie. The following modes were tested:

(1) Yttrium-88 source without overload pulses.

(2) Yttrium-88 source and 100× overload pulses in parallel to the signal input.

(3) Yttrium-88 source, with 100× overload pulses supplied to the shield input as well as to the signal input.

The results are given in Table 8. It can be seen that there is no observable effect of large pulses on either peak position or resolution. Mode 3 also served to verify the action of the shield for large input pulses. The large-amplitude counts in Modes 1 and 3 are due to the natural background; the large-amplitude count in Mode 2 does not include the major fraction of overload pulses which address above channel 255.

Table 8. Effect of veto action on spectral distribution (1.84-MeV peak of Y-88)

Mode	Peak position, channel	Resolution, %	Counts in peak channel	Large-amplitude counts
1	72.2	5.85	8527	18
2	72.1	5.77	7906	1254
3	72.1	5.84	8525	20

L. Pulse Pair Resolution

Among the features designed into the breadboard is a hazard gate which inhibits conversion of any event for a planned 13 μsec following the opening of the linear gate. The hazard gate is designed to prevent pulse pileup on the tail of a preceding pulse, an effect which becomes more probable with increasing incident flux. The operation of the hazard gate was observed on a dual-beam oscilloscope to be 11–12 μsec long for pulses of varying amplitude.

M. Digital Readout Logic and Scaler Functions

A sample of the computer program presentation of data transmitted through the digital readout logic is shown in Fig. 10. Following a line provided for identification, the veto, busy (i.e., reject), and shield scaler information is given for each frame of the run. Reading from left to right, the four columns of information for each scaler function are the occurrence of time to overflow bit, number of events in that frame, parity error indication, and rate in counts/sec. The scaler readout is in doubled columns for compactness. Below the words "lost sync" is a line showing the accumulation period of the run and the average rates of the three scaler functions for that particular period. Below this is the accumulated pulse-height analyzer data with 5 columns of information for each channel; these are, from left to right, channel number, number of events, the state of parity bit, the rate in counts/min, and the flux in counts/cm² sec keV. Whenever a PHA word contains no channel address, i.e., is all zeros, a "no" word is transmitted. The number of "no" words is given in the event column of channel 1.

In the sample shown in Fig. 10 (ID 126), a pulse rate of 300/sec was fed simultaneously to the signal and shield inputs. The energy per channel and "go" (geometry) entries have no physical significance in this example. Since veto is disabled, there are no counts in the veto scaler. The nonrandom input rate of 300 pulses/sec allows all the counts to be converted and transmitted so that the reject (busy) scaler is also empty. The shield scaler is counting 170–172 events/frame. Since the shield scaler is sampled for 0.286 sec/frame, this corresponds to an average of 599 counts/sec instead of the expected 300 counts/sec. This doubling of the proper rate is probably due to triggering on both edges of the input pulse. No parity errors are observed. The accumulation time is 59.9 sec, and the average shield rate is given as 600 counts/sec.

The number of events expected in the spectrum is the product of the input rate times the accumulation time times the fraction of conversion time per frame (the linear gate at the input gate of the ADC is closed during words 1–9 of each frame). For run 126 of Fig. 10 we expect (300) (59.9) (119/128) = 16,710. Channel 66 is observed to contain 16,734 events. The expected number of "no" events is given by the total number of words during the accumulation period minus the number of events transmitted:

$$\left[\frac{59.9 \text{ sec}}{2.3 \times 10^{-3} \text{ sec/event}}\left(\frac{119}{128}\right)\right] - 16{,}734 = 7478$$

Channel 1 has recorded 7421 events.

Eleven digital readout sequences were recorded, all using pulser inputs to the breadboard, under varying conditions of pulse rate, with and without shield input,

LUNAR ORBITER

300 PULSES/SEC   COINCIDENCE MODE

VETO DISABLE

IC 126   DATE 670203   TIME 162000   EN/CHAN 1.00 KEV   GO 1.000

	VETO	REJECT	SHIELD	VETO	REJECT	SHIELD
0	0 0 0.000E-38 • 0	0 0 0.000E-38 • 0	170 0 0.595E 03 • 0	0 0 0.000E-38 • 0	0 0 0.000E-38 • 0	172 0 0.602E 03 •
0	0 0 0.000E-38 • 0	0 0 0.000E-38 • 0	170 0 0.595E 03 • 0	0 0 0.000E-38 • 0	0 0 0.000E-38 • 0	172 0 0.602E 03 •
0	0 0 0.000E-38 • 0	0 0 0.000E-38 • 0	170 0 0.595E 03 • 0	0 0 0.000E-38 • 0	0 0 0.000E-38 • 0	172 0 0.602E 03 •
0	0 0 0.000E-38 • 0	0 0 0.000E-38 • 0	170 0 0.595E 03 • 0	0 0 0.000E-38 • 0	0 0 0.000E-38 • 0	172 0 0.602E 03 •
0	0 0 0.000E-38 • 0	0 0 0.000E-38 • 0	170 0 0.595E 03 • 0	0 0 0.000E-38 • 0	0 0 0.000E-38 • 0	172 0 0.602E 03 •
0	0 0 0.000E-38 • 0	0 0 0.000E-38 • 0	170 0 0.595E 03 • 0	0 0 0.000E-38 • 0	0 0 0.000E-38 • 0	172 0 0.602E 03 •
0	0 0 0.000E-38 • 0	0 0 0.000E-38 • 0	170 0 0.595E 03 • 0	0 0 0.000E-38 • 0	0 0 0.000E-38 • 0	172 0 0.602E 03 •
0	0 0 0.000E-38 • 0	0 0 0.000E-38 • 0	170 0 0.595E 03 • 0	0 0 0.000E-38 • 0	0 0 0.000E-38 • 0	172 0 0.602E 03 •
0	0 0 0.000E-38 • 0	0 0 0.000E-38 • 0	170 0 0.595E 03 • 0	0 0 0.000E-38 • 0	0 0 0.000E-38 • 0	172 0 0.602E 03 •
0	0 0 0.000E-38 • 0	0 0 0.000E-38 • 0	170 0 0.595E 03 • 0	0 0 0.000E-38 • 0	0 0 0.000E-38 • 0	172 0 0.602E 03 •
0	0 0 0.000E-38 • 0	0 0 0.000E-38 • 0	171 0 0.599E 03 • 0	0 0 0.000E-38 • 0	0 0 0.000E-38 • 0	172 0 0.602E 03 •
0	0 0 0.000E-38 • 0	0 0 0.000E-38 • 0	172 0 0.602E 03 • 0	0 0 0.000E-38 • 0	0 0 0.000E-38 • 0	172 0 0.602E 03 •
0	0 0 0.000E-38 • 0	0 0 0.000E-38 • 0	172 0 0.602E 03 • 0	0 0 0.000E-38 • 0	0 0 0.000E-38 • 0	172 0 0.602E 03 •
0	0 0 0.000E-38 • 0	0 0 0.000E-38 • 0	172 0 0.602E 03 • 0	0 0 0.000E-38 • 0	0 0 0.000E-38 • 0	172 0 0.602E 03 •
0	0 0 0.000E-38 • 0	0 0 0.000E-38 • 0	172 0 0.602E 03 • 0	0 0 0.000E-38 • 0	0 0 0.000E-38 • 0	172 0 0.602E 03 •
0	0 0 0.000E-38 • 0	0 0 0.000E-38 • 0	172 0 0.602E 03 • 0	0 0 0.000E-38 • 0	0 0 0.000E-38 • 0	172 0 0.602E 03 •
0	0 0 0.000E-38 • 0	0 0 0.000E-38 • 0	172 0 0.602E 03 • 0	0 0 0.000E-38 • 0	0 0 0.000E-38 • 0	172 0 0.602E 03 •
0	0 0 0.000E-38 • 0	0 0 0.000E-38 • 0	172 0 0.602E 03 • 0	0 0 0.000E-38 • 0	0 0 0.000E-38 • 0	172 0 0.602E 03 •
0	0 0 0.000E-38 • 0	0 0 0.000E-38 • 0	172 0 0.602E 03 • 0	0 0 0.000E-38 • 0	0 0 0.000E-38 • 0	172 0 0.602E 03 •
0	0 0 0.000E-38 • 0	0 0 0.000E-38 • 0	172 0 0.602E 03 • 0	0 0 0.000E-38 • 0	0 0 0.000E-38 • 0	172 0 0.602E 03 •
0	0 0 0.000E-38 • 0	0 0 0.000E-38 • 0	172 0 0.602E 03 • 0	0 0 0.000E-38 • 0	0 0 0.000E-38 • 0	172 0 0.602E 03 •
0	0 0 0.000E-38 • 0	0 0 0.000E-38 • 0	172 0 0.602E 03 • 0	0 0 0.000E-38 • 0	0 0 0.000E-38 • 0	172 0 0.602E 03 •
0	0 0 0.000E-38 • 0	0 0 0.000E-38 • 0	172 0 0.602E 03 • 0	0 0 0.000E-38 • 0	0 0 0.000E-38 • 0	172 0 0.602E 03 •
0	0 0 0.000E-38 • 0	0 0 0.000E-38 • 0	172 0 0.602E 03 • 0	0 0 0.000E-38 • 0	0 0 0.000E-38 • 0	172 0 0.602E 03 •
0	0 0 0.000E-38 • 0	0 0 0.000E-38 • 0	172 0 0.602E 03 • 0	0 0 0.000E-38 • 0	0 0 0.000E-38 • 0	172 0 0.602E 03 •
0	0 0 0.000E-38 • 0	0 0 0.000E-38 • 0	172 0 0.602E 03 • 0	0 0 0.000E-38 • 0	0 0 0.000E-38 • 0	172 0 0.602E 03 •
0	0 0 0.000E-38 • 0	0 0 0.000E-38 • 0	172 0 0.602E 03 • 0	0 0 0.000E-38 • 0	0 0 0.000E-38 • 0	172 0 0.602E 03 •
0	0 0 0.000E-38 • 0	0 0 0.000E-38 • 0	172 0 0.602E 03 • 0	0 0 0.000E-38 • 0	0 0 0.000E-38 • 0	172 0 0.602E 03 •
0	0 0 0.000E-38 • 0	0 0 0.000E-38 • 0	172 0 0.602E 03 • 0	0 0 0.000E-38 • 0	0 0 0.000E-38 • 0	172 0 0.602E 03 •
0	0 0 0.000E-38 • 0	0 0 0.000E-38 • 0	172 0 0.602E 03 • 0	0 0 0.000E-38 • 0	0 0 0.000E-38 • 0	172 0 0.602E 03 •
0	0 0 0.000E-38 • 0	0 0 0.000E-38 • 0	172 0 0.602E 03 • 0	0 0 0.000E-38 • 0	0 0 0.000E-38 • 0	172 0 0.602E 03 •
0	0 0 0.000E-38 • 0	0 0 0.000E-38 • 0	172 0 0.602E 03 • 0	0 0 0.000E-38 • 0	0 0 0.000E-38 • 0	172 0 0.602E 03 •
0	0 0 0.000E-38 • 0	0 0 0.000E-38 • 0	172 0 0.602E 03 • 0	0 0 0.000E-38 • 0	0 0 0.000E-38 • 0	172 0 0.602E 03 •
0	0 0 0.000E-38 • 0	0 0 0.000E-38 • 0	172 0 0.602E 03 • 0	0 0 0.000E-38 • 0	0 0 0.000E-38 • 0	172 0 0.602E 03 •
0	0 0 0.000E-38 • 0	0 0 0.000E-38 • 0	172 0 0.602E 03 • 0	0 0 0.000E-38 • 0	0 0 0.000E-38 • 0	172 0 0.602E 03 •
0	0 0 0.000E-38 • 0	0 0 0.000E-38 • 0	172 0 0.602E 03 • 0	0 0 0.000E-38 • 0	0 0 0.000E-38 • 0	172 0 0.602E 03 •
0	0 0 0.000E-38 • 0	0 0 0.000E-38 • 0	172 0 0.602E 03 • 0	0 0 0.000E-38 • 0	0 0 0.000E-38 • 0	172 0 0.602E 03 •
0	0 0 0.000E-38 • 0	0 0 0.000E-38 • 0	172 0 0.602E 03 • 0	0 0 0.000E-38 • 0	0 0 0.000E-38 • 0	172 0 0.602E 03 •
0	0 0 0.000E-38 • 0	0 0 0.000E-38 • 0	172 0 0.602E 03 • 0	0 0 0.000E-38 • 0	0 0 0.000E-38 • 0	172 0 0.602E 03 •
0	0 0 0.000E-38 • 0	0 0 0.000E-38 • 0	171 0 0.599E 03 • 0	0 0 0.000E-38 • 0	0 0 0.000E-38 • 0	172 0 0.602E 03 •
0	0 0 0.000E-38 • 0	0 0 0.000E-38 • 0	170 0 0.595E 03 • 0	0 0 0.000E-38 • 0	0 0 0.000E-38 • 0	172 0 0.602E 03 •
0	0 0 0.000E-38 • 0	0 0 0.000E-38 • 0	171 0 0.599E 03 • 0	0 0 0.000E-38 • 0	0 0 0.000E-38 • 0	172 0 0.602E 03 •
0	0 0 0.000E-38 • 0	0 0 0.000E-38 • 0	170 0 0.595E 03 • 0	0 0 0.000E-38 • 0	0 0 0.000E-38 • 0	172 0 0.602E 03 •
0	0 0 0.000E-38 • 0	0 0 0.000E-38 • 0	170 0 0.595E 03 • 0	0 0 0.000E-38 • 0	0 0 0.000E-38 • 0	172 0 0.602E 03 •
0	0 0 0.000E-38 • 0	0 0 0.000E-38 • 0	170 0 0.595E 03 • 0	0 0 0.000E-38 • 0	0 0 0.000E-38 • 0	172 0 0.602E 03 •
0	0 0 0.000E-38 • 0	0 0 0.000E-38 • 0	170 0 0.595E 03 • 0	0 0 0.000E-38 • 0	0 0 0.000E-38 • 0	172 0 0.602E 03 •
0	0 0 0.000E-38 • 0	0 0 0.000E-38 • 0	170 0 0.595E 03 • 0	0 0 0.000E-38 • 0	0 0 0.000E-38 • 0	172 0 0.602E 03 •
0	0 0 0.000E-38 • 0	0 0 0.000E-38 • 0	170 0 0.595E 03 • 0	0 0 0.000E-38 • 0	0 0 0.000E-38 • 0	172 0 0.602E 03 •
0	0 0 0.000E-38 • 0	0 0 0.000E-38 • 0	170 0 0.595E 03 • 0	0 0 0.000E-38 • 0	0 0 0.000E-38 • 0	172 0 0.602E 03 •
0	0 0 0.000E-38 • 0	0 0 0.000E-38 • 0	171 0 0.599E 03 • 0	0 0 0.000E-38 • 0	0 0 0.000E-38 • 0	172 0 0.602E 03 •
0	0 0 0.000E-38 • 0	0 0 0.000E-38 • 0	172 0 0.602E 03 • 0	0 0 0.000E-38 • 0	0 0 0.000E-38 • 0	172 0 0.602E 03 •
0	0 0 0.000E-38 • 0	0 0 0.000E-38 • 0	172 0 0.602E 03 • 0	0 0 0.000E-38 • 0	0 0 0.000E-38 • 0	172 0 0.602E 03 •
0	0 0 0.000E-38 • 0	0 0 0.000E-38 • 0	172 0 0.602E 03 • 0	0 0 0.000E-38 • 0	0 0 0.000E-38 • 0	172 0 0.602E 03 •
0	0 0 0.000E-38 • 0	0 0 0.000E-38 • 0	172 0 0.602E 03 • 0	0 0 0.000E-38 • 0	0 0 0.000E-38 • 0	172 0 0.602E 03 •
0	0 0 0.000E-38 • 0	0 0 0.000E-38 • 0	172 0 0.602E 03 • 0	0 0 0.000E-38 • 0	0 0 0.000E-38 • 0	172 0 0.602E 03 •
0	0 0 0.000E-38 • 0	0 0 0.000E-38 • 0	172 0 0.602E 03 • 0	0 0 0.000E-38 • 0	0 0 0.000E-38 • 0	172 0 0.602E 03 •
0	0 0 0.000E-38 • 0	0 0 0.000E-38 • 0	172 0 0.602E 03 • 0	0 0 0.000E-38 • 0	0 0 0.000E-38 • 0	172 0 0.602E 03 •
0	0 0 0.000E-38 • 0	0 0 0.000E-38 • 0	172 0 0.602E 03 • 0	0 0 0.000E-38 • 0	0 0 0.000E-38 • 0	172 0 0.602E 03 •

LOST SYNC

ACCUMULATION TIME 59.9 SEC OF 0.0 SEC   VETO 0.000E-38 0   REJECT 0.000E-38 0   SHIELD 0.600E 03 0 C/SEC

CHAN	EVENTS	PAR	RATE(C/MIN)	FLUX	CHAN	EVENTS	PAR	RATE(C/MIN)	FLUX
1	7421.	0	0.000E-38	0.000E-38	129	0.	0	0.000E-38	0.000E-38
2	1.	0	0.100E 01	0.167E-01	130	0.	0	0.000E-38	0.000E-38
3	0.	0	0.000E-38	0.000E-38	131	0.	0	0.000E-38	0.000E-38
4	0.	0	0.000E-38	0.000E-38	132	0.	0	0.000E-38	0.000E-38
5	0.	0	0.000E-38	0.000E-38	133	0.	0	0.000E-38	0.000E-38
6	0.	0	0.000E-38	0.000E-38	134	0.	0	0.000E-38	0.000E-38
7	1.	0	0.100E 01	0.167E-01	135	0.	0	0.000E-38	0.000E-38
8	0.	0	0.000E-38	0.000E-38	136	0.	0	0.000E-38	0.000E-38
9	0.	0	0.000E-38	0.000E-38	137	0.	0	0.000E-38	0.000E-38
10	0.	0	0.000E-38	0.000E-38	138	0.	0	0.000E-38	0.000E-38
11	0.	0	0.000E-38	0.000E-38	139	0.	0	0.000E-38	0.000E-38
12	0.	0	0.000E-38	0.000E-38	140	0.	0	0.000E-38	0.000E-38
13	0.	0	0.000E-38	0.000E-38	141	0.	0	0.000E-38	0.000E-38
14	0.	0	0.000E-38	0.000E-38	142	0.	0	0.000E-38	0.000E-38
15	0.	0	0.000E-38	0.000E-38	143	0.	0	0.000E-38	0.000E-38
16	0.	0	0.000E-38	0.000E-38	144	0.	0	0.000E-38	0.000E-38
17	0.	0	0.000E-38	0.000E-38	145	0.	0	0.000E-38	0.000E-38
18	0.	0	0.000E-38	0.000E-38	146	0.	0	0.000E-38	0.000E-38
19	0.	0	0.000E-38	0.000E-38	147	0.	0	0.000E-38	0.000E-38
20	0.	0	0.000E-38	0.000E-38	148	0.	0	0.000E-38	0.000E-38
21	0.	0	0.000E-38	0.000E-38	149	0.	0	0.000E-38	0.000E-38
22	0.	0	0.000E-38	0.000E-38	150	0.	0	0.000E-38	0.000E-38
23	0.	0	0.000E-38	0.000E-38	151	0.	0	0.000E-38	0.000E-38
24	0.	0	0.000E-38	0.000E-38	152	0.	0	0.000E-38	0.000E-38
25	0.	0	0.000E-38	0.000E-38	153	0.	0	0.000E-38	0.000E-38
26	0.	0	0.000E-38	0.000E-38	154	0.	0	0.000E-38	0.000E-38
27	0.	0	0.000E-38	0.000E-38	155	0.	0	0.000E-38	0.000E-38
28	0.	0	0.000E-38	0.000E-38	156	0.	0	0.000E-38	0.000E-38
29	0.	0	0.000E-38	0.000E-38	157	0.	0	0.000E-38	0.000E-38
30	0.	0	0.000E-38	0.000E-38	158	0.	0	0.000E-38	0.000E-38
31	0.	0	0.000E-38	0.000E-38	159	0.	0	0.000E-38	0.000E-38
32	0.	0	0.000E-38	0.000E-38	160	0.	0	0.000E-38	0.000E-38
33	0.	0	0.000E-38	0.000E-38	161	0.	0	0.000E-38	0.000E-38
34	0.	0	0.000E-38	0.000E-38	162	0.	0	0.000E-38	0.000E-38
35	0.	0	0.000E-38	0.000E-38	163	0.	0	0.000E-38	0.000E-38
36	0.	0	0.000E-38	0.000E-38	164	0.	0	0.000E-38	0.000E-38
37	0.	0	0.000E-38	0.000E-38	165	0.	0	0.000E-38	0.000E-38
38	0.	0	0.000E-38	0.000E-38	166	0.	0	0.000E-38	0.000E-38
39	0.	0	0.000E-38	0.000E-38	167	0.	0	0.000E-38	0.000E-38
40	0.	0	0.000E-38	0.000E-38	168	0.	0	0.000E-38	0.000E-38
41	0.	0	0.000E-38	0.000E-38	169	0.	0	0.000E-38	0.000E-38
42	0.	0	0.000E-38	0.000E-38	170	0.	0	0.000E-38	0.000E-38
43	0.	0	0.000E-38	0.000E-38	171	0.	0	0.000E-38	0.000E-38
44	0.	0	0.000E-38	0.000E-38	172	0.	0	0.000E-38	0.000E-38
45	0.	0	0.000E-38	0.000E-38	173	0.	0	0.000E-38	0.000E-38
46	0.	0	0.000E-38	0.000E-38	174	0.	0	0.000E-38	0.000E-38
47	0.	0	0.000E-38	0.000E-38	175	0.	0	0.000E-38	0.000E-38
48	0.	0	0.000E-38	0.000E-38	176	0.	0	0.000E-38	0.000E-38
49	0.	0	0.000E-38	0.000E-38	177	0.	0	0.000E-38	0.000E-38
50	0.	0	0.000E-38	0.000E-38	178	0.	0	0.000E-38	0.000E-38
51	0.	0	0.000E-38	0.000E-38	179	0.	0	0.000E-38	0.000E-38
52	0.	0	0.000E-38	0.000E-38	180	0.	0	0.000E-38	0.000E-38
53	0.	0	0.000E-38	0.000E-38	181	0.	0	0.000E-38	0.000E-38
54	0.	0	0.000E-38	0.000E-38	182	0.	0	0.000E-38	0.000E-38
55	0.	0	0.000E-38	0.000E-38	183	0.	0	0.000E-38	0.000E-38
56	0.	0	0.000E-38	0.000E-38	184	0.	0	0.000E-38	0.000E-38
57	0.	0	0.000E-38	0.000E-38	185	0.	0	0.000E-38	0.000E-38
58	0.	0	0.000E-38	0.000E-38	186	0.	0	0.000E-38	0.000E-38
59	0.	0	0.000E-38	0.000E-38	187	0.	0	0.000E-38	0.000E-38
60	0.	0	0.000E-38	0.000E-38	188	0.	0	0.000E-38	0.000E-38
61	0.	0	0.000E-38	0.000E-38	189	0.	0	0.000E-38	0.000E-38
62	0.	0	0.000E-38	0.000E-38	190	0.	0	0.000E-38	0.000E-38
63	0.	0	0.000E-38	0.000E-38	191	0.	0	0.000E-38	0.000E-38
64	0.	0	0.000E-38	0.000E-38	192	0.	0	0.000E-38	0.000E-38
65	0.	0	0.000E-38	0.000E-38	193	0.	0	0.000E-38	0.000E-38
66	16734.	0	0.168E 05	0.280E 03	194	0.	0	0.000E-38	0.000E-38
67	0.	0	0.000E-38	0.000E-38	195	0.	0	0.000E-38	0.000E-38
68	0.	0	0.000E-38	0.000E-38	196	0.	0	0.000E-38	0.000E-38
69	0.	0	0.000E-38	0.000E-38	197	0.	0	0.000E-38	0.000E-38
70	0.	0	0.000E-38	0.000E-38	198	0.	0	0.000E-38	0.000E-38
⋮									⋮
115	0.	0	0.000E-38	0.000E-38	243	0.	0	0.000E-38	0.000E-38
116	0.	0	0.000E-38	0.000E-38	244	0.	0	0.000E-38	0.000E-38
117	0.	0	0.000E-38	0.000E-38	245	0.	0	0.000E-38	0.000E-38
118	0.	0	0.000E-38	0.000E-38	246	0.	0	0.000E-38	0.000E-38
119	0.	0	0.000E-38	0.000E-38	247	0.	0	0.000E-38	0.000E-38
120	0.	0	0.000E-38	0.000E-38	248	0.	0	0.000E-38	0.000E-38
121	0.	0	0.000E-38	0.000E-38	249	0.	0	0.000E-38	0.000E-38
122	0.	0	0.000E-38	0.000E-38	250	0.	0	0.000E-38	0.000E-38
123	0.	0	0.000E-38	0.000E-38	251	0.	0	0.000E-38	0.000E-38
124	0.	0	0.000E-38	0.000E-38	252	0.	0	0.000E-38	0.000E-38
125	0.	0	0.000E-38	0.000E-38	253	0.	0	0.000E-38	0.000E-38
126	0.	0	0.000E-38	0.000E-38	254	0.	0	0.000E-38	0.000E-38
127	0.	0	0.000E-38	0.000E-38	255	0.	0	0.000E-38	0.000E-38
128	0.	0	0.000E-38	0.000E-38	256	0.	0	0.000E-38	0.000E-38

NO SYNC THIS RECORD

Fig. 10. Digital output format

coincidence mode, veto enable/disable, etc. The principal observations were as follows:

(1) With no input signal, no count accumulation was obtained in any function.

(2) With the veto disabled, the expected number of conversion pulses was seen in the proper channel of analysis.

(3) The number of "no" events tabulated in channel 1 agreed with predictions at all input rates.

(4) With the veto action enabled, a fraction of pulses was observed in the pulse-height analysis spectrum, indicating that the veto system was not inhibiting conversion with unit efficiency. Another test was made using a sodium iodide anticoincidence plastic scintillator detector. Cosmic ray events depositing 25 MeV or greater in the NaI crystal were counted in both the veto enable and veto disable modes. All such events should deposit enough energy in the plastic scintillator to prevent conversion in the HTC when the veto is enabled. The non-zero ratio of veto enable/veto disable (25%) confirmed a partial failure of the coincidence gating. To correct the problem, the length of the veto signal was extended to include the full period during which the linear gate is open. Subsequently, the functioning of the veto gate and the counting rate in the veto scaler were as expected.

(5) The shield rate was zero when not exercised, but when pulses were introduced into the shield amplifier and discriminator the rate was generally twice that expected. This suggested that the shield discriminator was triggering on the falling as well as the rising edge of the input pulse.

(6) When pulses were introduced simultaneously into the signal and shield inputs with veto enable (coincidence mode), a busy scaler count rate equal to the input rate was observed where none was expected. This was also observed when the veto was disabled. An error in logic seems to be the cause.

N. Miscellaneous

1. Veto threshold. Veto action was found to be initiated for a signal amplitude which would be converted to just above channel 3.2 in the ADC. For an energy range of 0–8.5 MeV this puts the veto discriminator at an energy equivalent of (3.2/256) (8.5) = 0.100 MeV, the level originally specified.

2. Veto action at high amplitudes. Veto action was maintained for pulse amplitudes equivalent to 50 MeV deposited in the scintillation plastic shield.

3. *Power.* The breadboard drew 37 mA at 33 V for a total power consumption of 1.22 W.

IV. Summary

The gamma ray spectrometer breadboard electronics designed by ATC have performed in a very satisfactory manner. The several malfunctions which were encountered during testing were not unexpected, particularly in view of the short time spent in system design and assembly. With two exceptions, these malfunctions were easily remedied. The remaining problems lie in the busy scaler and shield scaler functions, where there appear to be errors in digital design. It is expected that these errors will be corrected in the prototype which is now under construction. The final step in the development of a complete electronics system for this experiment will be the addition of a memory capability for data compression. A memory will be highly desirable for complete coverage of the lunar surface, and unless adequate onboard tape storage is available, it appears to be a necessity for any kind of planetary mission.

Appendix

Tests at the Oak Ridge National Laboratory

The tests performed on the breadboard at the Oak Ridge National Laboratory included the following:

1. Differential nonlinearity. This test was executed with a Berkeley Nuclear Corp. pulser model GL-3. The pulser was set for a 500-sec ramp period and an output pulse rate of 300/sec. The period of the run was 13¼ hr. The display is plotted in Fig. A-1. Channels 164 and 166 were observed to lose counts as the accumulated analysis was switched from the display to the readout mode and are neglected. The result gives a value of ±0.66%, with a trend to increasing channel widths. The effect is slight, however, and the nonlinearity is small.

2. Integral nonlinearity. This test was measured by the determination of 26 channel positions, with pulser values set manually so as to straddle channels in each case. The integral nonlinearity found was ±0.36 channels and ±0.14%.

3. Zero offset. Using the data of the previous test, the zero offset was found to be −2.049 channels.

4. Shield veto action. This test was performed with a breadboard of the proposed gamma ray spectrometer detector, a 2¾ × 2¾-in. sodium iodide (Tl) scintillation crystal surrounded on three sides by a ⅜-in. NE-102A scintillator plastic. The two scintillators are viewed by separate photomultiplier tubes. The source used to produce anticoincidence events was the beta emitter, yttrium-91. Each of the following runs was for 5 min:

(1) Veto enable: integral rate = 89.7 counts/sec.

(2) Veto disable: integral rate = 238 counts/sec.

(3) Shield input disconnected: integral rate = 238 counts/sec.

Spectra of the first two runs are shown in Fig. A-2. The counting rate with the veto enabled is not zero due to background counts, secondary photon production, and possible contamination in the source.

5. Cesium-137 spectrum. Source and background measurements were made for 10 min each. The integral background rate was 34 counts/sec; the integral Cs-137 rate was 110 counts/sec. Results (source minus background):

(a) Cs-137 peak resolution: 7.33%.

(b) Peak/valley ratio: 32.6.

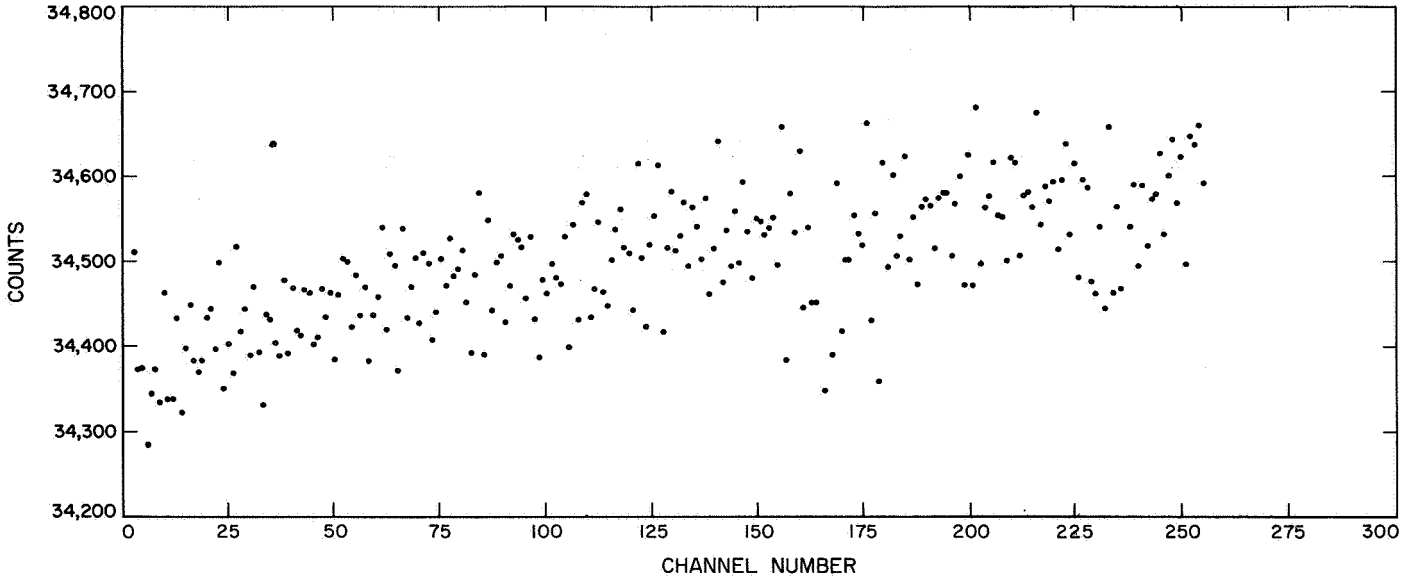

Fig. A-1. Differential linearity (II)

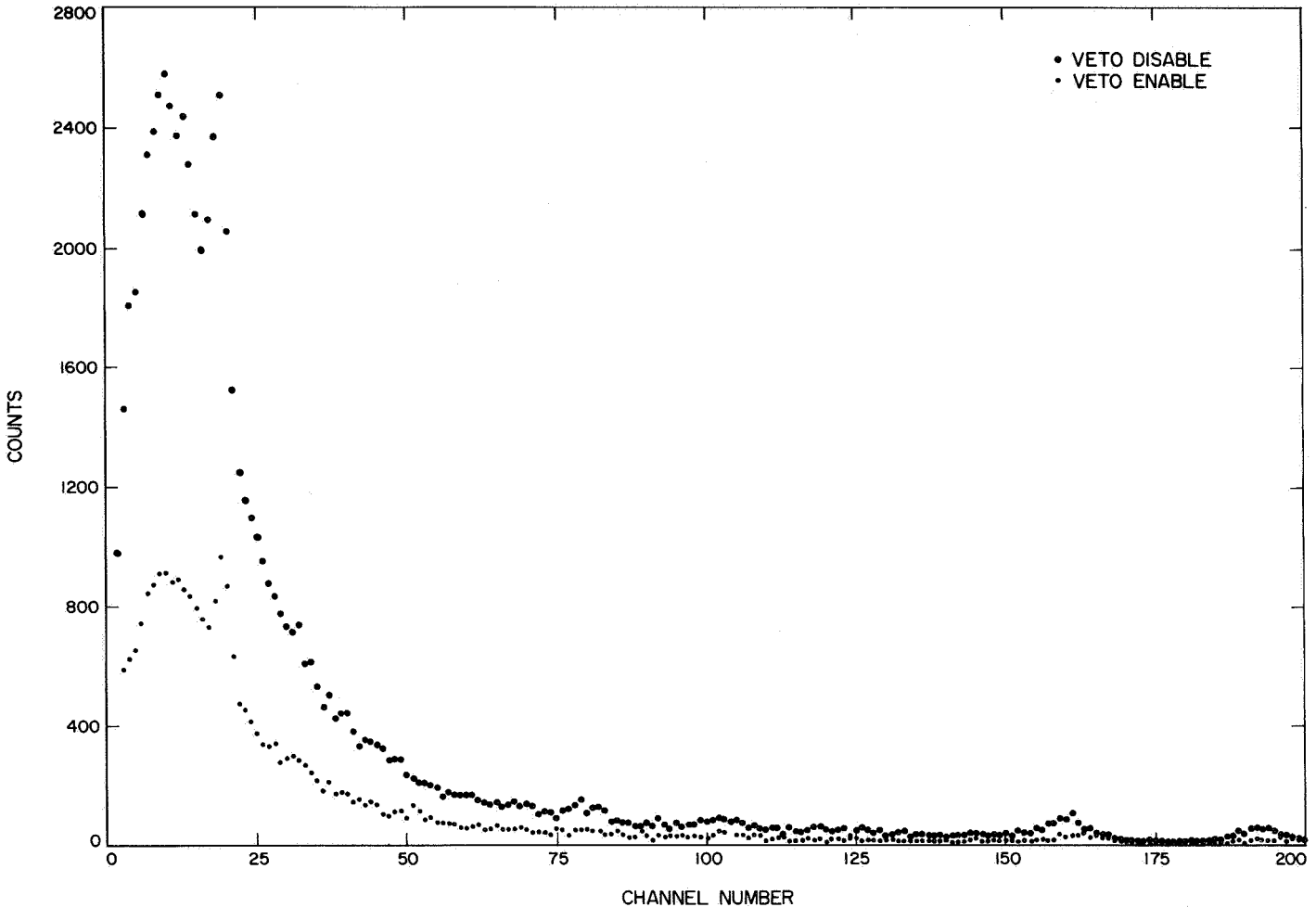

Fig. A-2. Veto action

6. Overload test. A source of Cs-137 irradiated the breadboard detector, which was connected in parallel to a source of overload pulses. The overload pulses were amplified to the equivalent of 118 MeV of energy deposited in the scintillation crystal at a frequency of 300 pulses/sec (rise time = 0 to 0.5 μsec, width of 2 μsec). Table A-1 shows that the effect of overload pulses on the electronics is negligible.

Table A-1. Overload recovery

	Peak position, channel	Resolution, %	Peak/valley
Cs-137 with overload pulses	99.72	7.13	16.1
Cs-137 without overload pulses	99.60	7.27	15.3

7. Count rate stability. A Harshaw integral line assembly consisting of a 3-in. NaI (Tl) crystal and an 8054 RCA photomultiplier tube was surrounded by 2 in. of lead. A Hammer high-voltage supply provided the high voltage for the photomultiplier tube. Two Co-60 sources, rated at approximately 0.5 μc and 8 μc were counted alternately under the same geometry. A pulser reference was used as a more sensitive monitor and to differentiate between effects due to the detector and the PHA. Four runs were made, each 10 min in length, and the results are shown in Table A-2. The pulser peak at the low

Table A-2. Count rate stability (II)

Run	Co-60 source, μc	Pulser setting, channel	Pulser position in display, channel	1.33 MeV peak position, channel	Peak position (1.332 MeV) / Peak position (1.173 MeV)
1	0.5	239.50	239.43	209.8	1.134
2	8	239.50	239.50	214.5	1.138
3	0.5	15.50	15.49	194.5	1.135
4	8	15.50	–	208.3	1.135

energy of the spectrum was swamped in conjunction with the high flux from the 8-μc Co-60 source; the pulser position which lay above the photopeak in run 2 was not affected up to a detector output rate of at least 8 kHz. The photopeak position is seen to have shifted significantly on runs 2 and 3. The 7% drop in run 3 is especially puzzling because this is one of the 0.5-μc activity tests. Unfortunately, the shift was not noted at the time of the measurement, but the contrasting stability of the pulser indicates a loose or faulty connection in the signal lines or possibly a problem in the laboratory high-voltage supply. The ratio of the 1.33 and 1.17 MeV Co-60 gamma ray photopeaks agrees with the literature value of 1.136 within 0.2%. Thus the linearity as well as the gain of the breadboard PHA is unaffected by a change in count rate over the range of the test, in agreement with the observations at JPL.